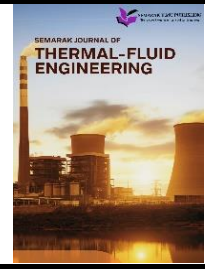




## Semarak Journal of Thermal-Fluid Engineering

Journal homepage:  
<https://semarakilmu.com.my/journals/index.php/sjotfe/index>  
ISSN: XXXX-XXXX



# Computational Modelling on Virus Spread Among People in Group

Ridwan Abdurrahman<sup>1</sup>, Lim Hong Yang<sup>2</sup>, Ishkrizat Taib<sup>2,\*</sup>, Muhammad Aniq Azarif<sup>2</sup>, Muhammad Naqib Ruslan<sup>2</sup>, Andril Arafat<sup>3</sup>

<sup>1</sup> Mechanical Engineering Department, Universitas Riau, Pekanbaru 28293, Indonesia

<sup>2</sup> Faculty of Mechanical Engineering, University of Tun Hussein Onn Malaysia, 86400 Parit Raja, Johor, Malaysia

<sup>3</sup> Department of Mechanical Engineering, Faculty of Engineering, Universitas Negeri Padang

### ARTICLE INFO

#### Article history:

Received 23 March 2024

Received in revised form 29 April 2024

Accepted 25 May 2024

Available online 12 June 2024

#### Keywords:

COVID-19; flow characteristic; velocity; pressure distribution

### ABSTRACT

The COVID-19 pandemic has made it necessary to recognise various transmission routes, including talking, as potential means of spreading the virus. Therefore, this study seeks to analyse the capability of COVID-19 virus particles to spread through talking, specifically focusing on the fluid contour and the characteristics of velocity and pressure during interpersonal communication. To compare the results, three experiments were conducted using three inlet velocities at the mouth of the pipe: 2.31 m/s, 3.19 m/s, and 4.07 m/s. These were combined with three group densities: 2-person, 3-person, and 4-person groups, using ANSYS Fluent software, resulting in nine cases in total. The findings revealed that the velocity rate of the flow was high during the initial stages of talking and declined with the distance of flow. The chances of virus transmission were higher in situations where participants interacted with more people, particularly when three patients with COVID-19 were conversing. From the study, it was established that virus transmission increases with the number of people talking and decreases with the distance between them in a conversation, which underlines the importance of social distancing.

## 1. Introduction

The COVID-19 pandemic, also known as the coronavirus pandemic, is an ongoing global pandemic of coronavirus disease 2019 (COVID-19) caused by severe acute respiratory syndrome coronavirus 2 (SARS-CoV-2). This novel virus was first identified in the Chinese city of Wuhan in December 2019. The lockdown in other cities surrounding Hubei failed to contain the outbreak. The World Health Organization (WHO) declared a Public Health Emergency of International Concern on 30 January 2020 and a pandemic on 11 March 2020. Multiple variants of the virus have emerged, led by alpha, beta, gamma, delta, and Omicron variants. As of 12 December 2021, more than 269 million cases and 5.3 million deaths have been confirmed, making the pandemic one of the deadliest in history [1, 2].

SARS-CoV-2 is a member of the Coronaviridae family and order Nidovirales. The family includes two subfamilies, Coronavirinae and Torovirinae. Members of the subfamily Coronavirinae are

\* Corresponding author.

E-mail address: [iszat@@uthm.edu.my](mailto:iszat@@uthm.edu.my)

<https://doi.org/10.37934/sjotfe.1.1.4356>

subdivided into four genera: (a) Alphacoronavirus, which includes the human coronavirus (HCoV)-229E and HCoV-NL63; (b) Betacoronavirus, which includes HCoV-OC43, severe acute respiratory syndrome human coronavirus (SARS-HCoV), HCoV-HKU1, and Middle Eastern respiratory syndrome coronavirus (MERS-CoV); (c) Gammacoronavirus, which consists of viruses of whales and birds; and (d) Deltacoronavirus, which consists of viruses isolated from pigs and birds [3].

According to literature, coughing, sneezing, talking, and breathing are the four primary mechanisms responsible for the formation of respiratory aerosol particles. The former two methods have larger numerical concentrations of released particles; hence, they are given more weight in determining transmission properties. As a result, most investigations have concentrated on coughing and sneezing [4, 5]. Asymptomatic individuals, who rarely cough or sneeze, are also known to spread disease vectors [6], which may contribute significantly to the total disease burden [7]. Consequently, a few recent studies have focused on the transfer of information during conversing [8]. Due to the differences in ejection characteristics, the distance travelled and the time spent in the aerosol plume differ for different respiratory processes.

Subsequently, the particle size, density, existing flow pattern, and initial velocity of exhaled/emitted particles influence the distance travelled by the aerosol particles. General interpretations based on threshold parameters, such as safe distance, are problematic in two-phase systems with transition dynamics. Respiratory droplets with diameters larger than 5  $\mu\text{m}$  have been shown to have a brief air residence period and settle at a distance of less than 1 m [9]. Asadi *et al.*, [4] mentioned that there are two possible modes of COVID-19 aerosol transmission: during a sneeze or a cough, "droplet sprays" of virus-laden respiratory tract fluid, typically greater than 5  $\mu\text{m}$  in diameter, directly impact a susceptible individual; alternatively, a susceptible person can inhale microscopic aerosol particles consisting of the residual solid components of evaporated respiratory droplets, which are sufficiently small ( $< 5 \mu\text{m}$ ) to remain airborne for hours.

However, in another study, droplets of the same size range were shown to be distributed over greater distances [10]. Such a wide range of outcomes is not surprising because of the interaction between the properties of the exhaled respiratory particles and the flow dynamics. Coronavirus clings to droplets/particles in the respiratory system and is released during coughing, sneezing, talking, and other activities. In a study by Chia *et al.*, [11], SARS-CoV-2-bearing particles with diameters  $> 4$  and  $14 \mu\text{m}$  were identified in air samples within airborne infection isolation rooms with 12 air changes per hour (ACH).

Regarding indoor transmission, ventilation conditions significantly impact aerosol movement and deposition as well as safe distancing. Guidelines have frequently emphasised the importance of ventilation as a crucial preventative and control measure [12]. The complex interplay between indoor ventilation fluid dynamics and expiration episodes in infected patients may influence disease-transmission mitigation strategies [13]. Poor ventilation design in various practical scenarios has been linked to inefficient particle removal, creation of local hot spots, and increased surface contamination [14]. Independent studies have indicated that airflow patterns are responsible for SARS-CoV-2 transmission through the air [15]. The complexity of airflow patterns also challenges threshold-based approaches for determining safe distances and deriving general meaning. Recent research has debated the ineffectiveness of a fixed safe distance, its dependence on external factors, and the recommendation to extend this distance beyond 2 m [16]. The relationship between airflow dynamics and particle transport in various indoor situations was studied and interpreted [17]. However, only a few comprehensive studies have examined all primary airborne transmission respiratory routes of transport vectors in an indoor setting.

COVID-19 spreads via airborne particles and droplets. Infected individuals can release particles and droplets containing the SARS-CoV-2 virus into the air when they exhale (e.g. quiet respiration,

speaking, singing, exercise, coughing, and sneezing) [18, 19]. Droplets or aerosol particles vary across a wide range of sizes from visible to microscopic. Once exhaled, these infectious droplets and particles move outwards from the person (the source). These droplets carry the virus and transmit the virus. Indoors, the finest droplets and particles continue to spread through the air in the room or space and can accumulate. COVID-19 is transmitted through contact with respiratory fluids that carry the SARS-CoV-2 virus. A person can be exposed to an infected individual by coughing or speaking near them. They can also be exposed by inhalation of aerosol particles that spread away from the infected person. Transmission of COVID-19 from inhalation of the virus in the air can occur at distances greater than six feet [20, 21]. Particles from an infected person can move throughout an entire room or indoor space. Air particles can also linger after a person has left the room, remaining airborne for hours in some cases. A person may also be exposed through splashes and sprays of respiratory fluids directly onto their mucous membranes. Spreading can also occur through contact with contaminated surfaces [22-25].

However, the World Health Organization states that the evidence is not compelling. Some virologists [4, 26] claim that the virus spreads only when patients cough or sneeze, releasing respiratory droplets that carry the virus and tiny particles (bioaerosols) containing SARS-CoV-2. The virus can remain suspended in the air in ultrafine mist produced when infected people exhale. Therefore, studies on how talking can spread the COVID-19 virus were conducted using CFD methods and the ANSYS Fluent software.

## 2. Methodology

### 2.1 Description of Model

The computational domain represented a typical indoor environment measuring 2.0 m in length, 2.0 m in width, and 2.6 m in height. This study simulated scenarios involving two, three, and four individuals at different inlet velocities. Figure 1 illustrates the detailed geometry of the computational space for each scenario. In the 2-person model (Figure 1(a)), two individuals are positioned at opposite ends of a rectangular space, each occupying a 1.0 m section. The 3-person model (Figure 1(b)) divides the length into three equal parts of approximately 0.67 m each, placing three individuals equidistantly. The 4-person model (Figure 1(c)) distributes four individuals evenly, with each occupying a 0.5 m section along the room's length. These configurations enabled a comprehensive analysis of how talking affects the flow of respiratory droplets with varying group sizes.

### 2.2 Discretization Technique

#### 2.2.1 Governing equation

The incompressible Reynolds-averaged Navier-Stokes (RANS) equation is solved using the computational fluid dynamics approach to derive the flow field of the face-to-face breathing droplet propagation region between sick and healthy individuals. The control equations were discretised using the finite volume method with the second-order upwind scheme for the discrete momentum equation, turbulent kinetic energy, and turbulent dissipation rate terms. The pressure equation was discretised using a second-order central scheme, and coupling of the velocity and pressure was achieved using the coupled method. The two-phase flow of breathing droplets following air is described by the Euler model of a multiphase flow. Eq. (1) expresses the air and droplet continuity equations:

$$\frac{\partial(a_k \rho_k)}{\partial t} + \nabla \cdot (a_k \rho_k U_k) = 0 \quad (1)$$

where  $\alpha$  is the volume fraction,  $U$  is the velocity vector (m/s), subscript  $k$  denotes a specific phase, subscript  $a$  represents the air phase, and subscript  $d$  represents the droplet phase. The droplet density and viscosity were assumed constant.

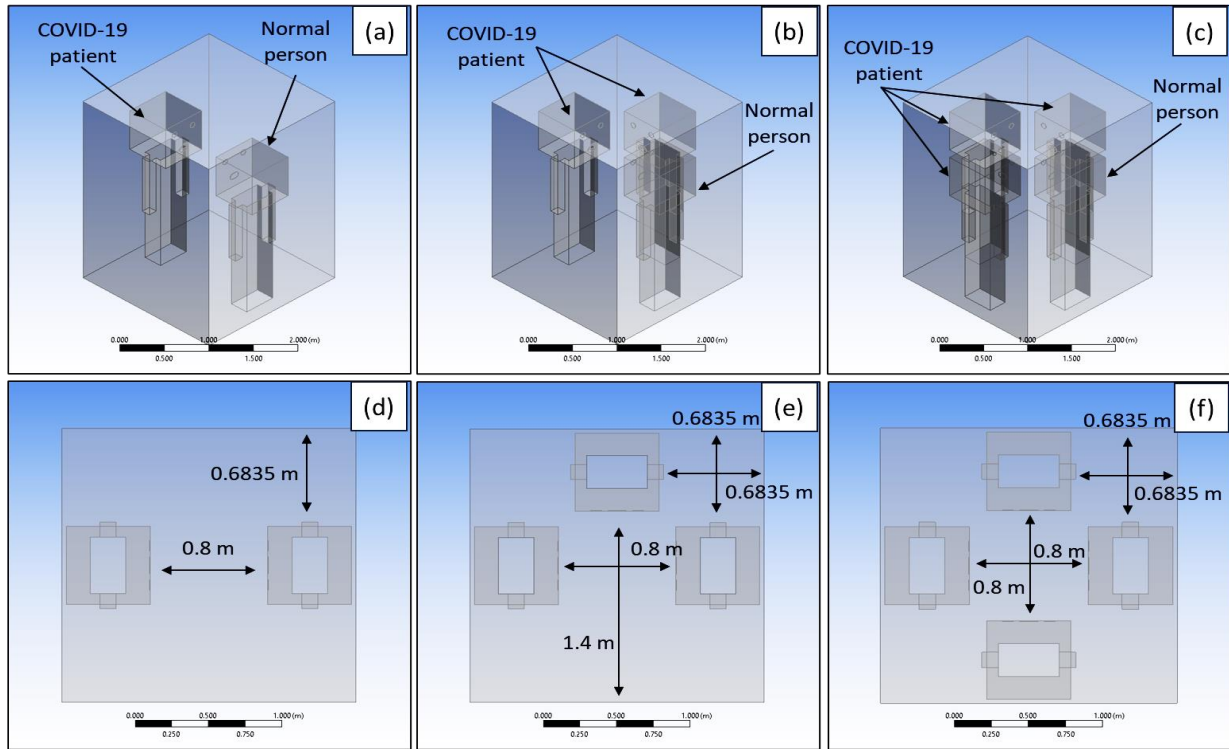


**Fig. 1.** Computational domain of (a) 2-person (b) 3-person and (c) 4-person. Top view of the distance with the boundary of computational for (d) 2-person (e) 3-person and (f) 4-person

The air momentum equation and droplet momentum equation are expressed as Eqs. (2) and (3), respectively.

$$\frac{\partial(a_a \rho_a U_a)}{\partial t} + \nabla \cdot (a_a \rho_a U_a U_a) = -a_a \nabla \rho + \nabla \cdot \tau_a + a_a \rho_a g + K(U_d - U_a) \quad (2)$$

$$\frac{\partial(a_d \rho_d U_d)}{\partial t} + \nabla \cdot (a_d \rho_d U_d U_d) = -a_d \nabla \rho + \nabla \cdot \tau_d + a_d \rho_d g + K(U_a - U_d) \quad (3)$$

This study employed the RNG k-turbulence model to represent turbulent flow, and the wall function approach was used to connect physical values along the wall with unknown quantities in the turbulent core area. The dimensionless distance between the node nearest to the wall and the wall was maintained within the range  $30 \leq y^+ \leq 300$ . The following form is used to explain the turbulence model equation:

$$\frac{\partial(\rho \phi_k)}{\partial t} + \nabla \cdot (\rho U_k \phi_k - \Gamma \phi_k \text{grad} \phi_k) = S \phi_k, k = 1, \dots, N \quad (4)$$

where  $\phi_k$  is a scalar,  $\Gamma \phi_k$  is the diffusion coefficient, and  $S \phi_k$  is the source term of the Nth scalar equation.

### 2.2.2 Meshing and parameter assumptions

The meshing process, performed using ANSYS Meshing, adheres to the constraints of ANSYS Fluent Student Version, which limits the number of elements and nodes to less than 512,000. The default element size of 0.19209 meters was refined to 0.06 meters to enhance accuracy. The mesh type was converted into tetrahedrons using the patch-conforming method. The total number of elements for the 2-person, 3-person, and 4-person models were 431,065, 432,125, and 430,853, respectively, with corresponding nodes of 78,168, 79,074, and 79,644, respectively, as shown in Figure 2. Key assumptions for the simulations include a constant density for the incompressible flow, steady-state conditions, no-slip wall conditions, and inviscid flow. Gravity effects were included with a gravitational acceleration of  $-9.81 \text{ m/s}^2$  along. The pressure-based solver settings are listed in Table 1.

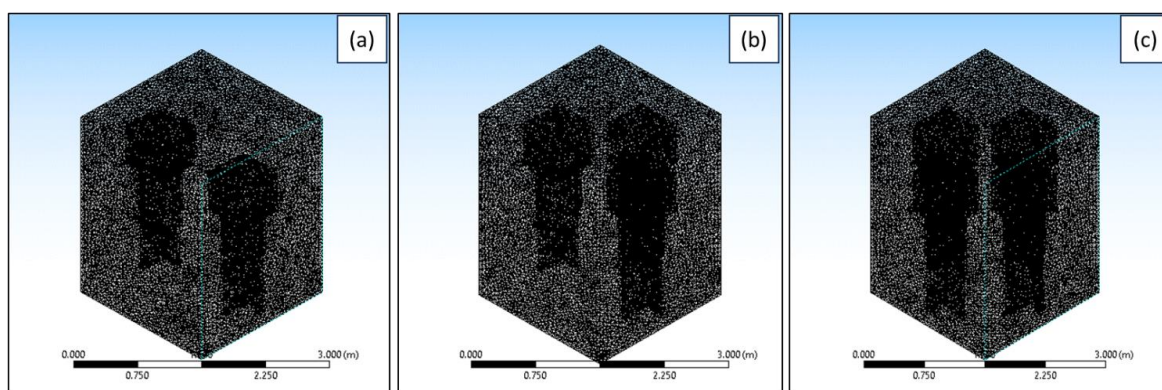


Fig. 2. Computational domain mesh of (a) 2-person (b) 3-person and (c) 4-person

**Table 1**

Simulation settings of meshing domain

Settings	
Viscous-k-epsilon	k-epsilon model: RNG Near-wall treatment: Standard wall function
Pressure-velocity coupling – Coupled	Pressure: Second order Momentum: Second order upwind Turbulent kinetic energy: Second order upwind Turbulent dissipation rate: Second order upwind Energy: Second order upwind
Initialization: Initialization methods – Standard	Gauge pressure: 0 Pascal Velocity magnitude: $0 \text{ m.s}^{-1}$ Temperature: 300 K

### 2.2.3 Boundary condition

The boundary conditions are crucial for defining the interaction between the computational domain and its environment. Table 2 summarises the key boundary conditions used in this study. The surrounding boundaries were defined as pressure outlets with a gauge pressure of 0 Pa and temperature of 300 K. The talking source at the mouth is modeled as a velocity inlet with velocities of 2.31 m/s, 3.19 m/s, and 4.07 m/s, and a temperature of 310 K. The floor and bodies were treated as stationary walls, with a heat flux of  $0 \text{ W/m}^2$ .

**Table 2**  
 Simulation setting of boundary condition

Settings	
Surrounding – Pressure outlet	Pressure gauge: 0 Pascal Backflow total temperature: 300 K
Mouth – Velocity inlet	Velocity magnitude: 2.31 m/s, 3.19 m/s or 4.07 m/s Temperature: 310 K
Floor and bodies – Wall	Wall motion: Stationary wall Heat flux: 0 W.m <sup>-2</sup>

### 3. Results

#### 3.1 Grid Independency Test (GIT)

The grid independence test ensured that the simulation results were not significantly affected by mesh size. This test involved refining the mesh and comparing the outcomes until the changes in the solution became negligible. Table 3 presents the results of the grid independence test, confirming that the final mesh configuration provided convergent and reliable results. For instance, the total number of nodes and elements for the 2-person, 3-person, and 4-person models demonstrates consistent behaviour across different mesh densities, indicating that further refinement would not substantially alter the results.

**Table 3**  
 GIT results of computational domain meshing

No.	Nodes	Elements	Convergence
2-Person			
1	77457	427343	No
2	77769	429113	No
3	78168	431065	Yes
3-person			
1	78288	427435	No
2	78635	429781	No
3	79074	432125	Yes
4-person			
1	78889	426703	No
2	79359	429287	No
3	79644	430853	Yes

#### 3.2 Simulation Results

In the 2-person scenario with an inlet velocity of 2.31 m/s, the simulation illustrated the propagation of respiratory droplets from both individuals, as shown in Figure 3. The droplets dispersed primarily in the airflow direction, with a significant interaction between the two streams. The velocity of the droplets was the highest near the mouths of the individuals and decreased as the distance increased. The highest concentration of droplets was observed within the first 0.5 meters from the source, indicating a high risk of transmission in close proximity. At an increased inlet velocity of 3.19 m/s, the droplets travelled further before settling (Figure 4). A higher velocity enhances the mixing and turbulence, resulting in a more complex flow pattern. The droplets covered a larger area, with notable dispersion up to 1.5 m from the source. This suggests that higher speaking velocities can increase the potential spread of respiratory droplets, emphasising the need to maintain an adequate physical distance in indoor settings.

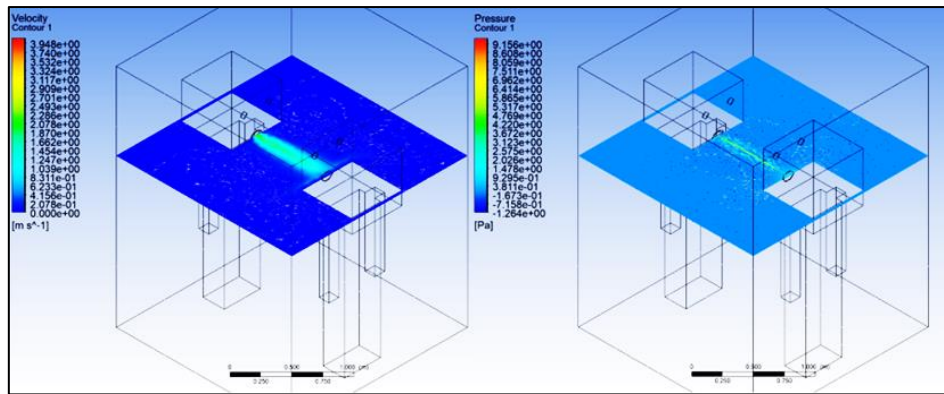


Fig. 3. 2-person with inlet velocity 2.31 m/s

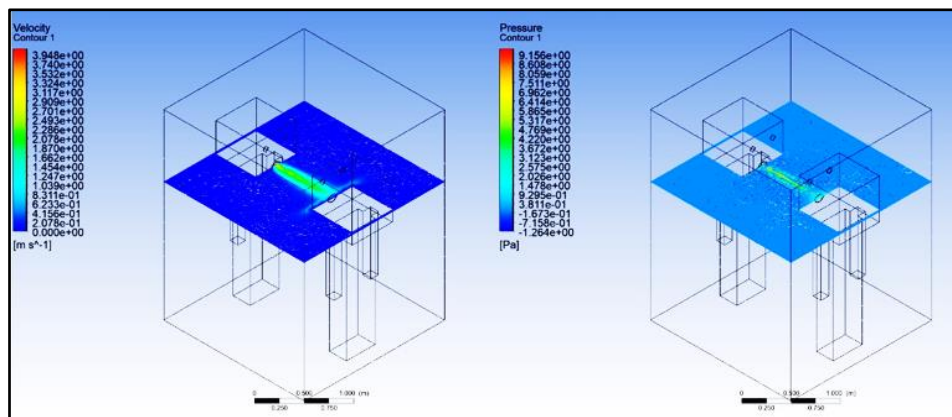


Fig. 4. 2-person with inlet velocity 3.19 m/s

When the inlet velocity was further increased to 4.07 m/s, the droplets dispersed even more widely (Figure 5). The simulation shows that droplets can travel up to 2 m before their velocity decreases significantly. The increased dispersion area and complexity of the flow field demonstrate that talking at higher velocities can substantially elevate the risk of virus transmission, making it crucial to control the speaking volume and airflow in shared spaces. In the 3-person scenario with an inlet velocity of 2.31 m/s, the droplets from the central person interacted with those from the adjacent individuals, creating a more intricate flow field (Figure 6). The droplets of the central person are dispersed in multiple directions, resulting in a significant overlap of the droplet paths. This interaction increases the risk of transmission among individuals standing close to each other, highlighting the importance of spacing to prevent cross-infection.

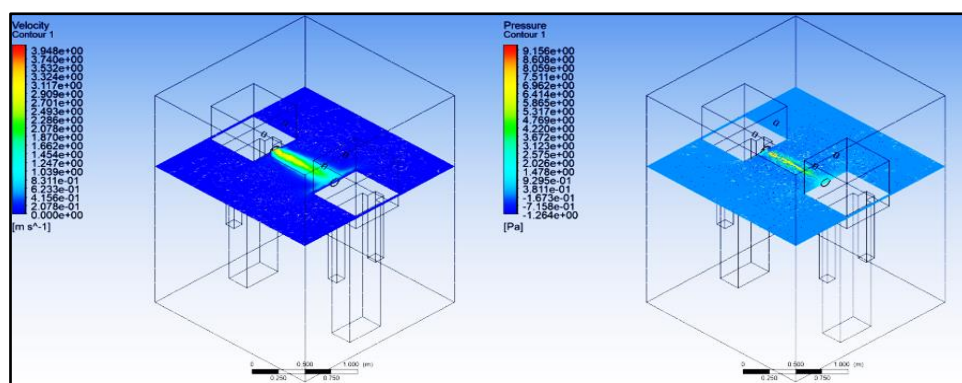


Fig. 5. 2-person with inlet velocity 4.07 m/s

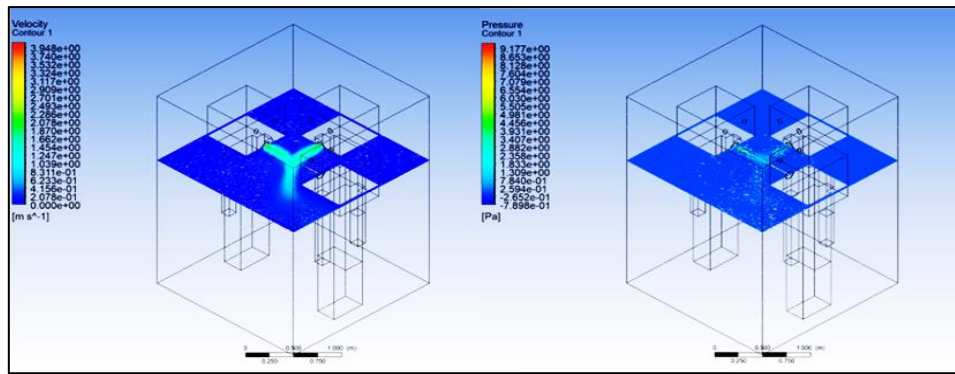


Fig. 6. 3-person with inlet velocity 2.31 m/s

At a higher inlet velocity of 3.19 m/s, the interaction between the droplets from all three individuals becomes more pronounced, as shown in Figure 7. The droplets travelled further, and the mixing zone expanded. The results indicate that the droplets can disperse up to 1.8 m from the source, with a high concentration observed within the first meter. This expansion of the interaction zone underscores the necessity for enhanced ventilation and air purification in indoor environments to mitigate transmission risks. At the highest velocity of 4.07 m/s (Figure 8), the droplets disperse widely, with a significant overlap between the streams from each individual. The complexity of the flow field increases, and the droplets can travel up to 2.2 m. This scenario highlights the critical need for effective airflow management to minimise the transmission of respiratory droplets in densely occupied spaces, especially where individuals talk loudly or for extended periods.

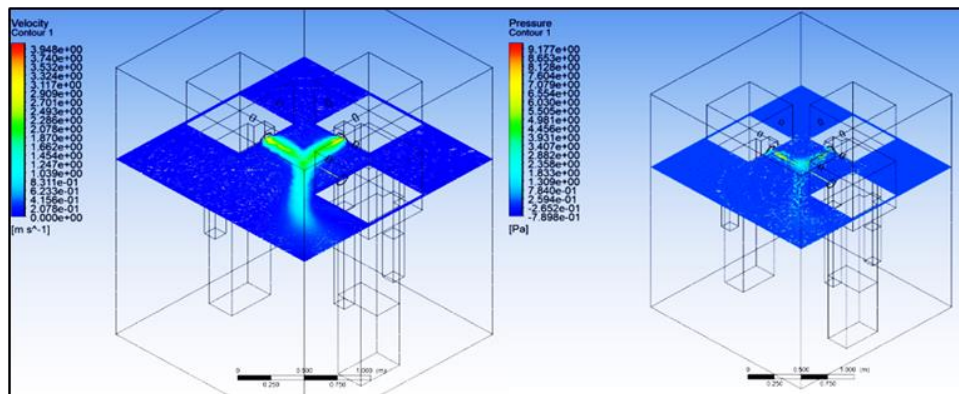


Fig. 7. 3-person with inlet velocity 3.19 m/s

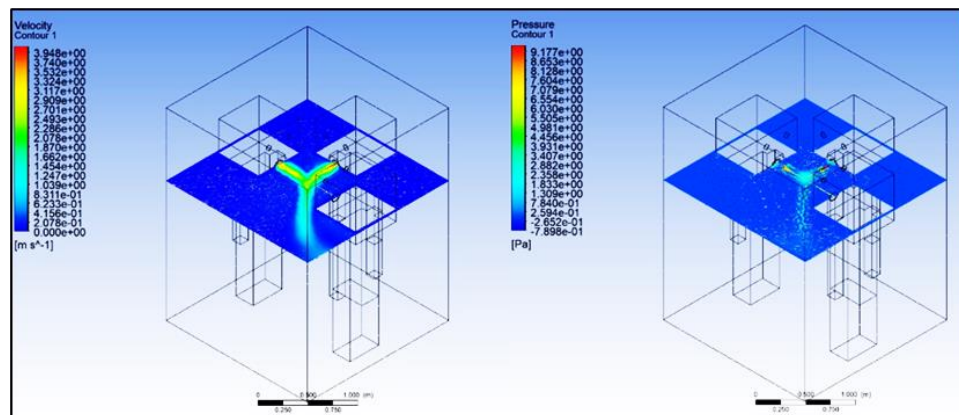


Fig. 8. 3-person with inlet velocity 4.07 m/s



In the 4-person scenario with an inlet velocity of 2.31 m/s, droplets from each individual interacted with those from others, creating a highly complex flow field (Figure 9). The dispersion pattern shows significant mixing and overlapping of droplets, with the highest concentration observed within 0.5 m from each source. The results emphasise the importance of physical barriers and spacing in reducing the risk of transmission in multiperson settings. A higher velocity results in more extensive dispersion and mixing. The droplets travel further, with a noticeable spread up to 1.5 m from each source. The interaction zones expand, indicating an increased risk of transmission in spaces where multiple individuals speak. The results highlight the need for the strategic placement of individuals and effective ventilation systems to control droplet spread (Figure 10).

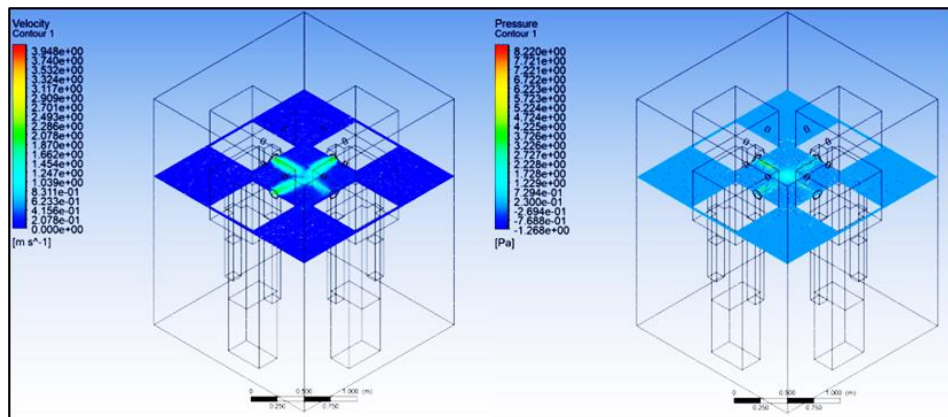


Fig. 9. 4-person with inlet velocity 2.31 m/s

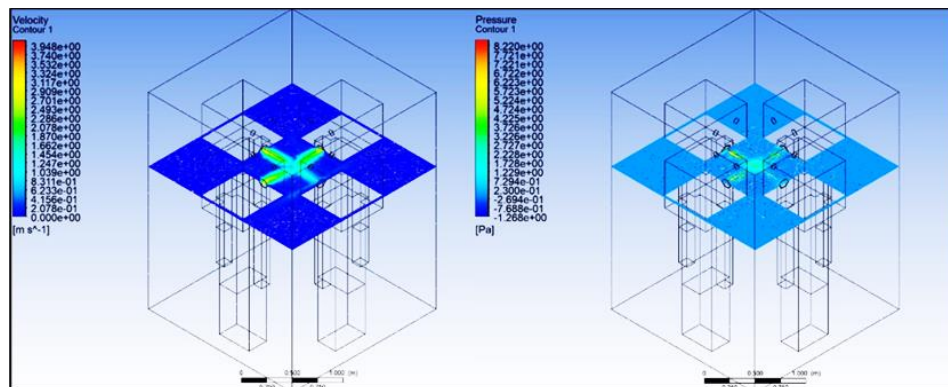


Fig. 10. 4-person with inlet velocity 3.19 m/s

At the highest velocity, the flow field becomes extremely complex, with the droplets dispersing widely and interacting with those from all individuals. The simulation showed that droplets can travel up to 2.2 m, significantly increasing the transmission risk. This scenario underscores the critical importance of maintaining low speaking volumes and ensuring robust ventilation to reduce the risk of airborne transmission in indoor environments, as shown in Figure 11.

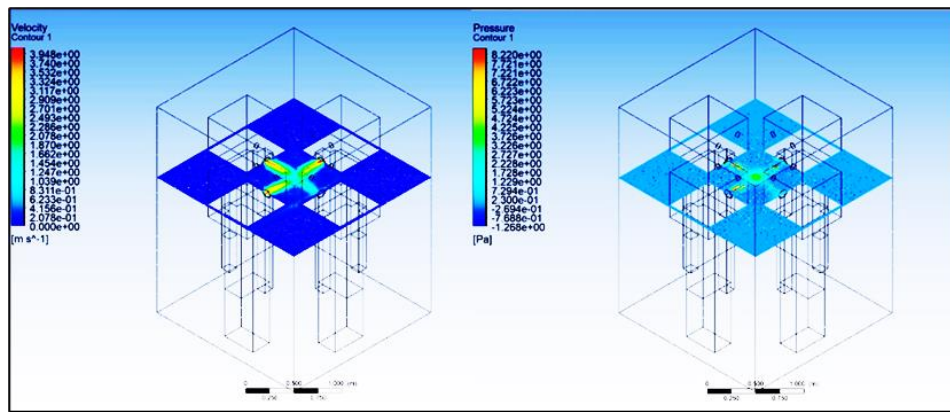


Fig. 11. 4-person with inlet velocity 4.07 m/s

Figure 12 shows the velocity chart of the differences in airflow patterns and velocities for the various scenarios. The highest velocities were observed near the mouths of individuals, which decreased with distance. The chart highlights how higher speaking velocities lead to more extensive droplet dispersion, indicating the influence of airflow on the transmission risk. The highest velocities are recorded in the 4-person scenario at a 4.07 m/s inlet velocity, showing the potential for widespread droplet dispersion in such configurations.

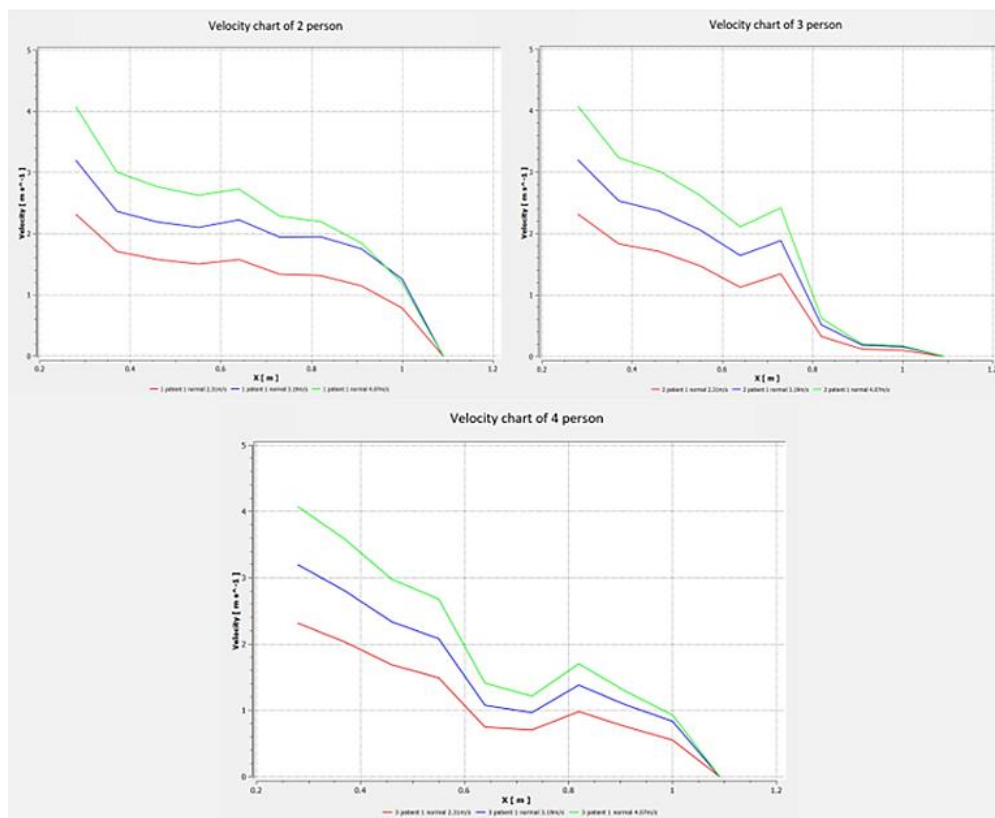


Fig. 12. Velocity chart of 2-person, 3 person and 4-person

The pressure chart shows the pressure distribution within the computational domain (Figure 13). Variations in pressure affect airflow patterns and, consequently, the dispersion of respiratory droplets. Higher pressures near the source mouths corresponded to higher velocities and a more significant droplet spread. The lowest pressures were observed at the pressure outlets, facilitating the outwards movement of the air and droplets.

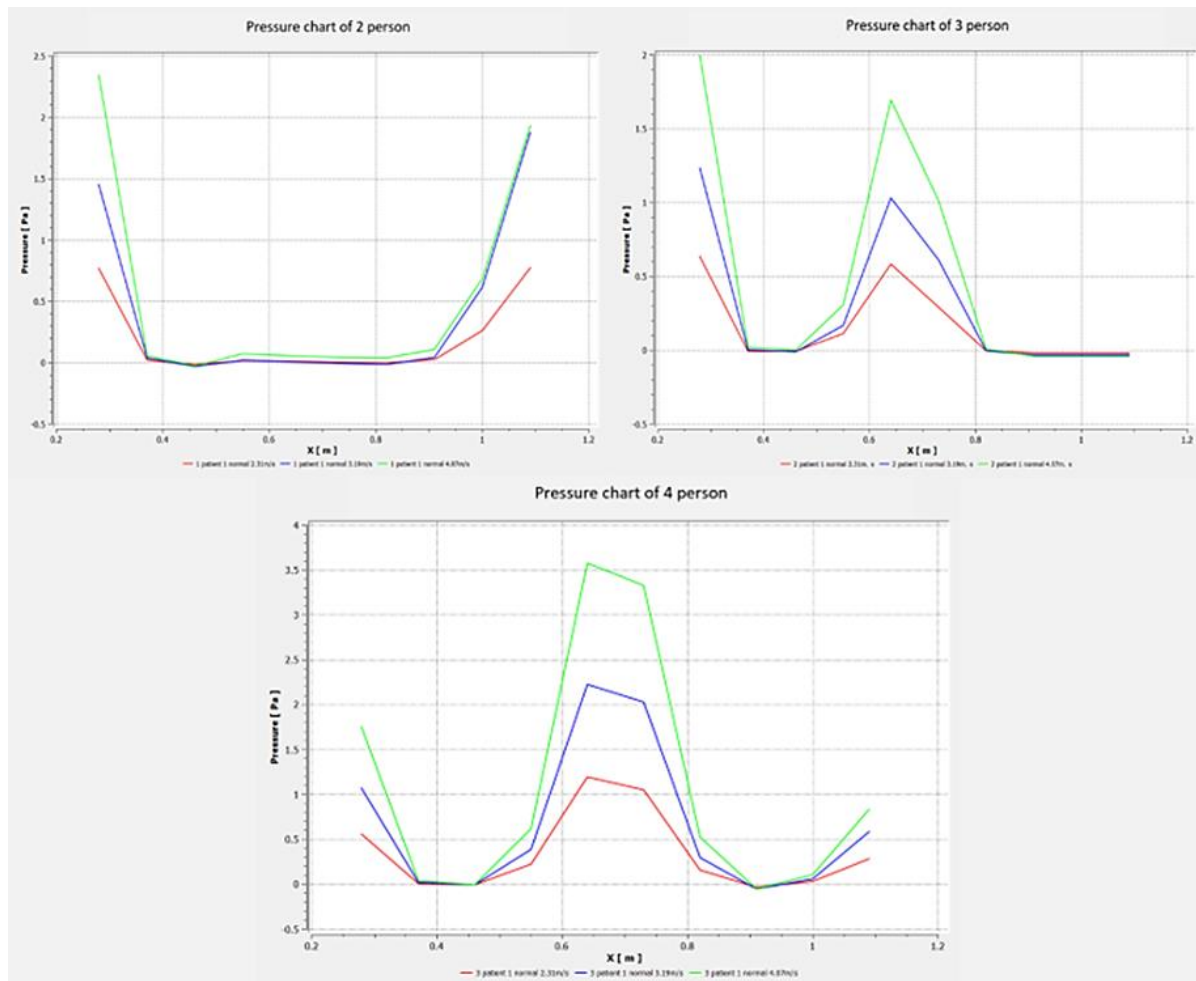


Fig. 13. Pressure chart of 2-person, 3 person and 4-person

### 3.3 Validation of Results

Validation of the simulation results is crucial for ensuring accuracy and reliability. The velocity trends observed in Figure 14 align with those recorded in previous studies, indicating that the simulation accurately captured the flow characteristics of respiratory droplets. The similarities in the velocity patterns between the current study and prior research confirm the validity of the simulation. Despite variations in specific parameters, the overall behaviour of the airflow and droplet dispersion was consistent with the established data, providing confidence in the findings of the study.

To further validate the results of this study, the jet characteristics observed in the simulation were compared with those from prior research, as shown in Figure 15. The jet patterns, velocity profiles, and dispersion characteristics in the simulation closely matched those reported in previous studies, reinforcing the credibility of the findings. The consistency between the simulated and experimental data demonstrated that the computational model effectively represented the physical phenomena of droplet propagation and interaction in indoor environments.

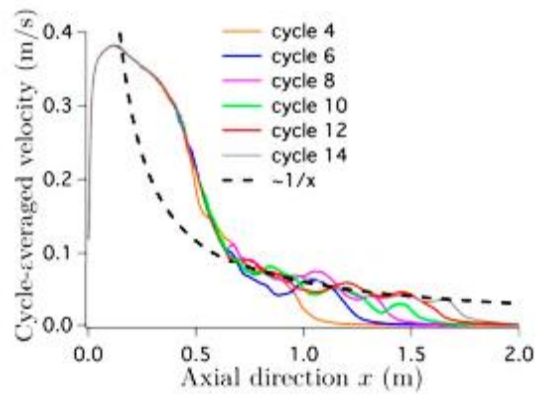


Fig. 14. Result of velocity chart [27]

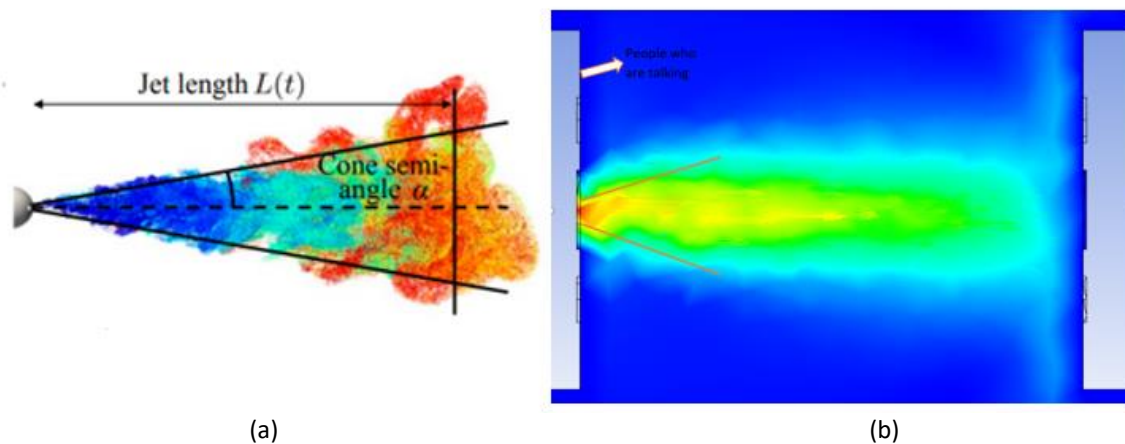


Fig. 15. Simulation result of jet characteristic (a) Previous study [27] (b) Current study

#### 4. Conclusions

In conclusion, the objectives of this project have been successfully achieved. The ability of virus particles to propagate has been determined by analysing the flow region (contour) of the fluid and fluid flow characteristics (velocity and pressure distribution) during interpersonal communication. This was accomplished using a CFD approach and ANSYS Fluent software. After completing the simulations, the flow characteristics for the three cases with three different inlet velocities were obtained. The velocity charts for the three cases showed consistent trends in the flow velocity. The velocity of the flow exiting the mouth was initially the highest but decreased to zero as the virus spread through the surrounding area along the distance. In the pressure charts, the flow pressure increased as the flow velocity decreased. By comparing all three cases, it can be concluded that the probability of a healthy person being infected by the virus was the highest when four individuals, including three COVID-19 patients, were talking simultaneously in the surrounding area. Through validation using previous studies, it was demonstrated that the simulations in this project were conducted successfully.

#### Acknowledgement

This research was supported by the Ministry of Higher Education (MOHE) through the Fundamental Research Grant Scheme (FRGS) (FRGS/1/2022/TK10/UTHM/03/5).

## References

- [1] Huang, Chaolin, Yeming Wang, Xingwang Li, Lili Ren, Jianping Zhao, Yi Hu, Li Zhang et al. "Clinical features of patients infected with 2019 novel coronavirus in Wuhan, China." *The lancet* 395, no. 10223 (2020): 497-506. [https://doi.org/10.1016/S0140-6736\(20\)30183-5](https://doi.org/10.1016/S0140-6736(20)30183-5)
- [2] Liu, Yen-Chin, Rei-Lin Kuo, and Shin-Ru Shih. "COVID-19: The first documented coronavirus pandemic in history." *Biomedical journal* 43, no. 4 (2020): 328-333. <https://doi.org/10.1016/j.bj.2020.04.007>
- [3] Hughes, James M., Mary E. Wilson, Stephen P. Luby, Emily S. Gurley, and M. Jahangir Hossain. "Transmission of human infection with Nipah virus." *Clinical infectious diseases* 49, no. 11 (2009): 1743-1748. <https://doi.org/10.1086/647951>
- [4] Ningthoujam, Ramananda. "COVID 19 can spread through breathing, talking, study estimates." *Current medicine research and practice* 10, no. 3 (2020): 132. <https://doi.org/10.1016/j.cmrp.2020.05.003>
- [5] Feng, Yu, Thierry Marchal, Ted Sperry, and Hang Yi. "Influence of wind and relative humidity on the social distancing effectiveness to prevent COVID-19 airborne transmission: A numerical study." *Journal of aerosol science* 147 (2020): 105585. <https://doi.org/10.1016/j.jaerosci.2020.105585>
- [6] Katelaris, Anthea L., Jessica Wells, Penelope Clark, Sophie Norton, Rebecca Rockett, Alicia Arnott, Vitali Sintchenko, Stephen Corbett, and Shopna K. Bag. "Epidemiologic evidence for airborne transmission of SARS-CoV-2 during church singing, Australia, 2020." *Emerging infectious diseases* 27, no. 6 (2021): 1677. <https://doi.org/10.3201/eid2706.210465>
- [7] Johansson, Michael A., Talia M. Quandelacy, Sarah Kada, Pragati Venkata Prasad, Molly Steele, John T. Brooks, Rachel B. Slayton, Matthew Biggerstaff, and Jay C. Butler. "SARS-CoV-2 transmission from people without COVID-19 symptoms." *JAMA network open* 4, no. 1 (2021): e2035057-e2035057. <https://doi.org/10.1001/jamanetworkopen.2020.35057>
- [8] Stadnytskyi, Valentyn, Christina E. Bax, Adriaan Bax, and Philip Anfinrud. "The airborne lifetime of small speech droplets and their potential importance in SARS-CoV-2 transmission." *Proceedings of the National Academy of Sciences* 117, no. 22 (2020): 11875-11877. <https://doi.org/10.1073/pnas.200687411>
- [9] Kutter, Jasmin S., Monique I. Spronken, Pieter L. Fraaij, Ron AM Fouchier, and Sander Herfst. "Transmission routes of respiratory viruses among humans." *Current opinion in virology* 28 (2018): 142-151. <https://doi.org/10.1016/j.coviro.2018.01.001>
- [10] Fernstrom, Aaron, and Michael Goldblatt. "Aerobiology and its role in the transmission of infectious diseases." *Journal of pathogens* 2013, no. 1 (2013): 493960. <https://doi.org/10.1155/2013/493960>
- [11] Chia, Po Ying, Kristen Kelli Coleman, Yian Kim Tan, Sean Wei Xiang Ong, Marcus Gum, Sok Kiang Lau, Xiao Fang Lim et al. "Detection of air and surface contamination by SARS-CoV-2 in hospital rooms of infected patients." *Nature communications* 11, no. 1 (2020): 2800. <https://doi.org/10.1038/s41467-020-16670-2>
- [12] Pendar, Mohammad-Reza, and José Carlos Páscoa. "Numerical modeling of the distribution of virus carrying saliva droplets during sneeze and cough." *Physics of Fluids* 32, no. 8 (2020). <https://doi.org/10.1063/5.0018432>
- [13] Bourouiba, Lydia. "The fluid dynamics of disease transmission." *Annual Review of Fluid Mechanics* 53 (2021): 473-508. <https://doi.org/10.1146/annurev-fluid-060220-113712>
- [14] Shao, Siyao, Dezhi Zhou, Ruichen He, Jiaqi Li, Shufan Zou, Kevin Mallery, Santosh Kumar, Suo Yang, and Jiarong Hong. "Risk assessment of airborne transmission of COVID-19 by asymptomatic individuals under different practical settings." *Journal of aerosol science* 151 (2021): 105661. <https://doi.org/10.1016/j.jaerosci.2020.105661>
- [15] Li, Yuguang, Hua Qian, Jian Hang, Xuguang Chen, Pan Cheng, Hong Ling, Shengqi Wang et al. "Probable airborne transmission of SARS-CoV-2 in a poorly ventilated restaurant." *Building and environment* 196 (2021): 107788. <https://doi.org/10.1016/j.buildenv.2021.107788>
- [16] Dbouk, Talib, and Dimitris Drikakis. "On coughing and airborne droplet transmission to humans." *Physics of Fluids* 32, no. 5 (2020). <https://doi.org/10.1063/5.0011960>
- [17] Lu, Jianyun, Jieni Gu, Kuibiao Li, Conghui Xu, Wenzhe Su, Zhisheng Lai, Deqian Zhou, Chao Yu, Bin Xu, and Zhicong Yang. "COVID-19 outbreak associated with air conditioning in restaurant, Guangzhou, China, 2020." *Emerging infectious diseases* 26, no. 7 (2020): 1628. <https://doi.org/10.3201/eid2607.200764>
- [18] Srivastava, Nishi. "Review of the Role of Aerosols in the Spread of COVID-19." In *Aerosol Optical Depth and Precipitation: Measuring Particle Concentration, Health Risks and Environmental Impacts*, pp. 177-188. Cham: Springer Nature Switzerland, 2024. [https://doi.org/10.1007/978-3-031-55836-8\\_10](https://doi.org/10.1007/978-3-031-55836-8_10)
- [19] Sarkar, Subendu, Rajender Pal Singh, and Gorachand Bhattacharya. "Effect of wet deposition on the transmission of aerosolized SARS-CoV-2: Facts and mechanisms." *International journal of Complementary and Internal Medicine* 6, no. 1 (2024): 268-275. <http://ijcimjournal.com/index.php/1/article/view/56>.
- [20] Khatibi, Elina Armani, Nastaran Farshbaf Moghimi, and Elaheh Rahimpour. "COVID-19: An overview on possible transmission ways, sampling matrices and diagnosis." *BiolImpacts* 14, no. 6 (2024): 29968-29968.

- [21] Oh, Wonseok, Ryoza Ooka, Hideki Kikumoto, and Sihwan Lee. "Effects of ventilation rate and social distancing on risk of transmission of disease: a numerical study using Eulerian-Lagrangian method." *Aerosol Science and Technology* 58, no. 1 (2024): 70-90. <https://doi.org/10.1080/02786826.2023.2271954>
- [22] Stadnytskyi, Valentyn, Christina E. Bax, Adriaan Bax, and Philip Anfinrud. "The airborne lifetime of small speech droplets and their potential importance in SARS-CoV-2 transmission." *Proceedings of the National Academy of Sciences* 117, no. 22 (2020): 11875-11877. <https://doi.org/10.1073/pnas.2006874117>
- [23] Alsved, Malin, Alexios Matamis, Ragnar Bohlin, Mattias Richter, P-E. Bengtsson, C-J. Fraenkel, Patrik Medstrand, and Jakob Löndahl. "Exhaled respiratory particles during singing and talking." *Aerosol Science and Technology* 54, no. 11 (2020): 1245-1248. <https://doi.org/10.1080/02786826.2020.1812502>
- [24] Echternach, Matthias, Sophia Gantner, Gregor Peters, Caroline Westphalen, Tobias Benthous, Bernhard Jakubaß, Liudmila Kuranova, Michael Döllinger, and Stefan Kniesburges. "Impulse dispersion of aerosols during singing and speaking: a potential COVID-19 transmission pathway." *American Journal of Respiratory and Critical Care Medicine* 202, no. 11 (2020): 1584-1587. <https://doi.org/10.1164/rccm.202009-3438LE>
- [25] Asadi, Sima, Anthony S. Wexler, Christopher D. Cappa, Santiago Barreda, Nicole M. Bouvier, and William D. Ristenpart. "Aerosol emission and superemission during human speech increase with voice loudness." *Scientific reports* 9, no. 1 (2019): 1-10.
- [26] National Academies of Sciences, Engineering, and Medicine. "Rapid expert consultation on the possibility of bioaerosol spread of SARS-CoV-2 for the COVID-19 pandemic (April 1, 2020)." (2020). <https://doi.org/10.17226/25769>
- [27] Abkarian, Manouk, Simon Mendez, Nan Xue, Fan Yang, and Howard A. Stone. "Speech can produce jet-like transport relevant to asymptomatic spreading of virus." *Proceedings of the National Academy of Sciences* 117, no. 41 (2020): 25237-25245. <https://doi.org/10.1073/pnas.201215611>